Ann. Telecommun. (2013) 68:57–62
DOI 10.1007/s12243-012-0313-z

Beam steering for wireless optical links based on an optical phased array in silicon

Hamdam Nikkhah · Karel Van Acoleyen · Roel Baets

Received: 30 November 2011 / Accepted: 29 May 2012 / Published online: 15 June 2012
© Institut Mines-Télécom and Springer-Verlag 2012

Abstract The ability to steer optical beams, crucial to the operation of high-speed optical wireless links may be achieved using optical phased array antennas which have significant potential in this application. The beam formed by the phased array antennas is steered by tuning the relative phase difference between the adjacent antenna elements which may be achieved nonmechanically. In this paper, the characteristics and behaviour of two dimensional optical phased arrays with a structure composed of 2×2, 4×4, and 16×16 antenna elements in beam steering are verified. The wavelength beam steering of −0.16°/nm is measured along the θ direction with a required steering range (between main lobes) of 1.97° within a −3 dB envelop of 5° extent in the θ direction and 7° extent in the Φ direction. To achieve two-dimensional beam steering, thermo-optic beam steering can be used in Φ direction. It is found that the thermo-optic phase tuning departs the expected quadratic dependence and is well characterised by a quartic dependence upon heater current or voltage.

Keywords Beam steering · Wireless optical links · Optical-phased array · Si Planar Light Circuit

H. Nikkhah (✉)
School of Electronic Engineering & Computer Science,
Centre for Research in Photonics, University of Ottawa,
800 King Edward Avenue,
Ottawa, ON K1N 6N5, Canada
e-mail: hnikk057@uottawa.ca

K. Van Acoleyen · R. Baets
Photonics Research Group, Ghent University-Interuniversity
MicroElectronics Centre,
Sint-Pietersnieuwstraat 41,
9000 Ghent, Belgium

1 Introduction

The maximum data rate in a wireless communication link is inversely proportional to the transmission loss. Hence, highly directional antennas are required at the transmitter and receiver antennas to minimise the loss and therefore maximise the capacity of the communication channel. Once link is established, it is important to maintain the link by tracking any relative motion of the transmitter, beam and receiver. This leads to a requirement for a sophisticated acquisition, pointing and tracking beam formation capability. One of the structures that have an important application in beam forming and beam steering in all-optical wireless communication systems, optical switching and optical sensing is optical phased array (OPA) antennas. The structure of an OPA consists of a collection of antenna elements that by tuning the relative phase difference between the adjacent elements on the array, the radiated beam from the array antenna can be steered to a desired angle.

Optical wireless communications find their importance when the limited bandwidth in the radio frequency spectrum becomes a serious problem in high-speed wireless communication systems. Optical phased arrays (OPAs) are rapid, precise and with a high gain in beam steering in contrast to the slow beam steering capability of bulky opto-mechanical beam steering devices these days [1]. The fully integrated OPA in a silicon-based material platform has the advantage of compactness and potentially low cost [2]. Phase tuning is possible in this implementation by using fixed delay lines combined with wavelength tuning or by exploiting the thermo-optic effect using waveguide sections equipped with electrical heating elements [3]. The two-dimensional beam steering can be achieved by combination of the both methods [2].

2 Structures and the characteristics

The silicon on insulator (SOI) platform provides high index contrast waveguide circuits and consequently offers the compact component footprints needed for dense integrated circuits. Compatibility with standard CMOS processing also eases manufacture. This choice results in grating couplers playing a significant role as one of the most efficient ways for interfacing between high-index contrast-integrated optical circuits and free space or an optical fibre. Figure 1 shows a schematic of a 4×4 structure with the elements consisting of 1D focusing diffractive grating couplers fabricated on SOI photonic integration platform [2, 4]. In this paper, the results of measurements are reported on structures consisting of 2×2, 4×4, and 16×16 two-dimensional arrays of antenna elements. The SOI oxide thickness is 2 μm. The silicon top layer thickness is 220 nm and the etching depth is 70 nm on this layer to make the grating coupler and 220 nm to make the waveguide and multimode interference splitters [2].

3 Far-field radiation pattern of the array antennas and its characteristics

In this experiment, the far-field radiation pattern of the OPAs is obtained in the rear focal plane of a microscope objective. This plane is then imaged for onto the sensor of a lens-less infrared camera using a telescope relay [2, 6] for image data capture. The far-field radiation patterns and their characteristics are defined by different factors on the chip such as number and size of the elements and the distance between the centres of the neighbouring elements [5]. Figure 2 shows the far-field radiation pattern of a 2×2 OPA on the IR camera at the wavelength 1,550 nm with the spacing of 45 μm

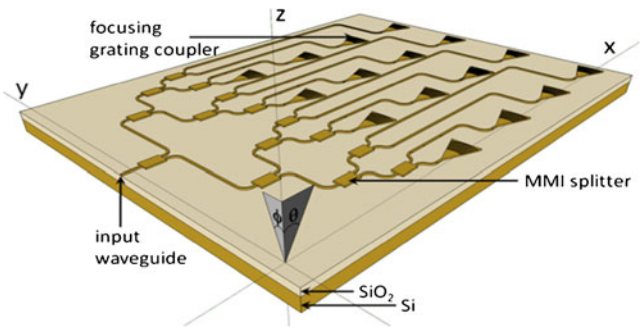

Fig. 1 Schematic of a 4×4 OPA on SOI, with the grating couplers as antenna elements [2]

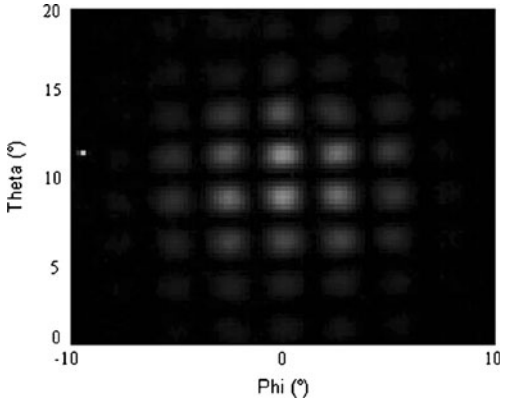

Fig. 2 Measured far field radiation pattern at the wavelength of 1,550 nm of a 2×2 OPA

between the elements in the θ direction and 35 μm in the Φ direction.

The beam width of the grating lobes for an operating vacuum wavelength of λ can be obtained from:

$$\Delta\theta_{\mathrm{FWHM}} \approx \frac{0.886\lambda}{N\Lambda\cos\theta} \tag{1}$$

where $\Delta\theta_{\mathrm{FWHM}}$ is the full width half maximum beam width, N is the number of elements, Λ is the distance between the elements, and θ is the angular position of the grating lobe, all measured along the relevant dimension of the array. This relation shows that the beam width of the grating lobes is in inverse proportion to the overall size of the array aperture and also the spacing between the elements [3, 7].

Referring to Eq. 1, the theoretical values of the beam widths in the θ direction, for the structures with the distance between the elements of 45 μm, are obtained as 0.87°, 0.43°, and 0.11° for 2×2, 4×4, and 16×16 OPAs, respectively; while the measured beam widths were found to be 0.90°, 0.58°, and not measurable for 16×16, respectively. The discrepancy between the theoretical values and the measured values increases with the number of elements in the structure. This is due to the experimental uncertainty in the measurement as the width of lobes of the 4×4 and 16×16 structures become narrower in comparison to the to the size of the pixels of the image sensor.

4 Wavelength beam steering

The far-field radiation pattern of optical array antennas is described by a number of factors, the most important of which is the array factor [8]. The array factor accounts for the effect of the array geometry independent of the radiation

pattern of an individual element. In the present case, it takes the form [2]:

$$T(\theta,\Phi)=\sum_{m=0}^{M-1}\sum_{n=0}^{N-1}A_{\mathrm{mn}}e^{-\mathrm{j}\beta_{\mathrm{mn}}}e^{K.S_{\mathrm{mn}}} \tag{2}$$

where K is the wave vector, A_{mn} is the amplitude, and β_{mn} is the phase of the signal received or driving the individual element indexed by (n, m) with position vector S_{mn}. Hence:

$$K.S_{\mathrm{mn}}=k_0\left(m\Lambda_x\sin\theta+n\Lambda_y\sin\Phi\right) \tag{3}$$

The phase delay for a structure with a waveguide delay section of length ΔL_{mn} is [2]:

$$\beta_{\mathrm{mn}}=n_{\mathrm{eff}}\frac{2\pi}{\lambda}\Delta L_{\mathrm{mn}} \tag{4}$$

where n_{eff} is the effective index for the TE-like fundamental mode of the waveguide. It indicates that the change in wavelength brings a change in the relative phase of the adjacent elements: a process referred to as "phase tuning". This results in beam steering if the delay sections are chosen as:

$$\Delta L_{\mathrm{mn}}=m\Delta L \tag{5}$$

The angles at which the peaks in the array factor occur can be obtained from [2]:

$$\sin\theta=\frac{q\lambda}{\Lambda}+n_{\mathrm{eff}}\frac{\Delta L}{\Lambda} \tag{6}$$

and hence the rate of change of the steered angle in θ with wavelength is [2]:

$$\frac{d\sin\theta}{d\lambda}=\frac{q}{\Lambda}+\frac{\mathrm{dn_{eff}}}{d\lambda}\frac{\Delta L}{\Lambda} \tag{7}$$

where Λ is the spacing between the elements and q is the order of the delay and is negative in the case of the calculations in this paper.

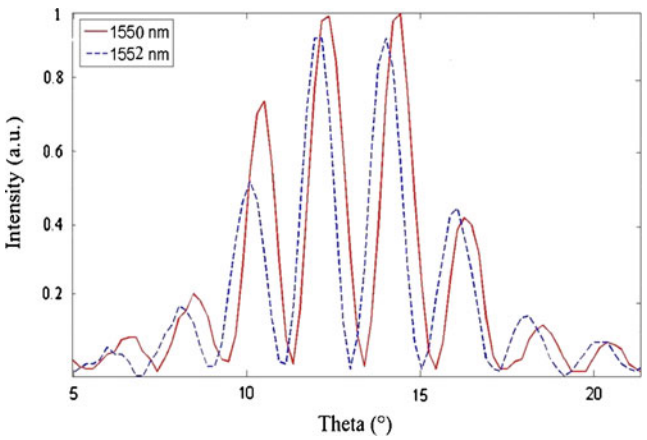

Fig. 3 Shift of the far-field pattern in 2×2 OPA by changing the wavelength from 1,550 to 1,552 nm

The far-field radiation pattern is given by the product of the array factor and the far-field radiation pattern of an individual antenna element (grating coupler). Figure 3 shows the measured far field radiation pattern of a 2×2 OPA that is steered by changing the wavelength from 1,550 to 1,552 nm. The calculation of the steering rate of −0.16°/nm in the far-field radiation pattern of this 2×2 structure with the spacing between the elements of 45 and 47 μm delay line increments is in agreement with the experimentally observed value of −0.16°/nm [9].

Similar measurements for a 4×4 structure with the same element spacing and delay line increments of 2×2 in the θ direction yield a value for the steering rate of −0.17°/nm. The discrepancy is again due to the experimental uncertainty in the measurement of the position of beams with narrower beam widths. The free-spectral range defines the maximum steering range of the grating lobes required and is predicted by theory to be 1.97°, which agrees nicely with the value measured for 2×2 and 4×4 OPAs structures [9]. Also as was mentioned previously, the beams are steered under an envelope given by the radiation pattern of the individual elements. This yields a −3 dB coverage range close to 5° in the θ direction and 7° in Φ direction, that correspond to a solid angle of 0.003π sr. The beam steering can be completed in two dimensions by using another method in orthogonal direction, for example using thermo-optic phase modulation sections, which offer a rapid and efficient steering mechanism referred to as thermo-optic phase tuning [4].

5 Thermo-optic beam steering

Materials with a refractive index with a high temperature coefficient of change have the potential to be employed to implement thermo-optic phase tuning. A heating element causes a large refractive index change without optical loss by changing the temperature of such waveguide material of which silicon is one that is particularly suitable in view of its high thermo-optic coefficient [10].

$$\frac{\mathrm{dn}}{\mathrm{dT}}=1.84.10^{-4}\mathrm{K}^{-1}@\lambda=1.5\mu\mathrm{m} \tag{8}$$

Here, n is the refractive index of silicon and T is temperature. The thermo-optic phase modulators are implemented by placing heater elements over a section of the waveguides that are connected to the antenna elements. The temperature of the heater is raised by injecting current or applying voltage to the heater elements and consequently the refractive index of the waveguides changes according to the relation (8). Consequently, change in the phase of the associated antenna element within the array factor is affected.

On-chip waveguide Mach–Zehnder interferometer (MZI) test structures provide an effective means to characterise the

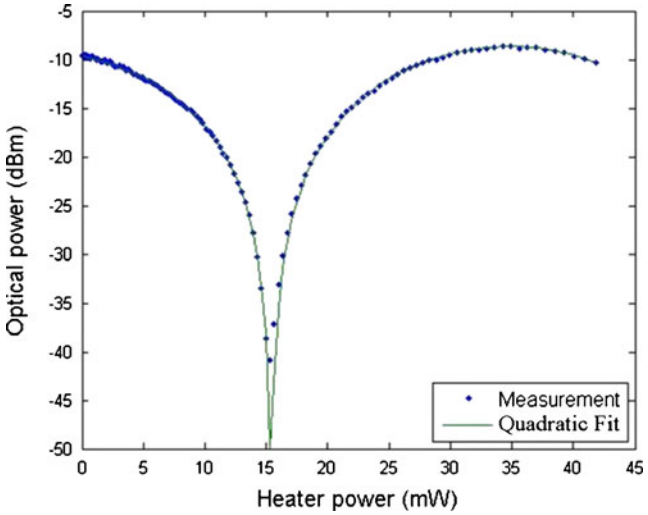

Fig. 4 Transmittance of a MZI vs. heater power. Optical power transmission (decibels per milliwatt) vs. heater power (milliwatts)

behaviour waveguide thermo-optic phase shifting elements. In the MZI, if the optical path lengths of the two arms are different, then there is a phase difference between the two beams which recombine at the output waveguide according to the principles of wave interference. If the phase difference is an even multiple of π, the interference of the two beams is constructive and the transmission of a lossless device is unity. But if the phase difference is an odd multiple of π, the interference of the two beams is destructive and the transmission of a lossless device is zero.

By changing the refractive index of one arm, it is possible to change the relative optical path length between the two arms. This can be done using a heater element which is placed over the waveguide of one arm. By applying an electric current through the element and using the Joule law, the temperature of the heater is changed and consequently the refractive index of the waveguide and the optical path length change which yields a phase difference between the two arms in the MZI.

The phase change is proportional to the refractive index change, which is described by Eq. 9 and is proportional to temperature change. Assuming thermal equilibrium, the temperature rise is proportional to the power dissipated by the

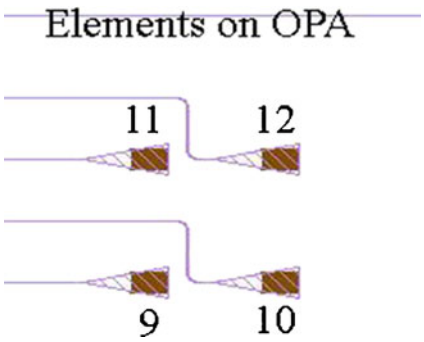

Fig. 5 The elements on a 2×2 OPA

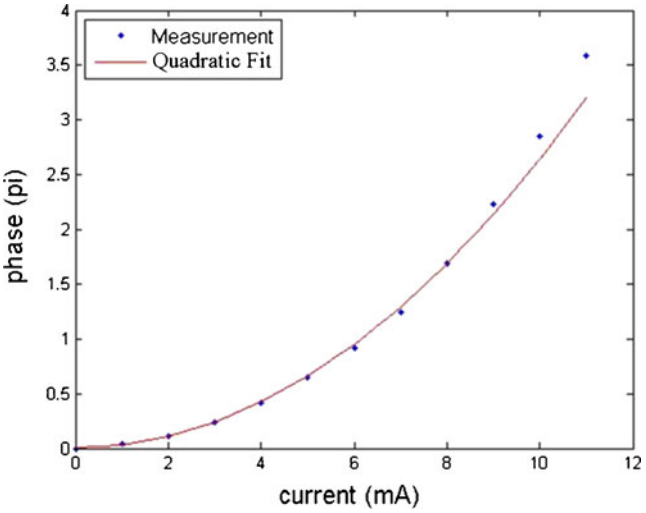

Fig. 6 The curve shows the relation between induced phase and heater current (milliampere) for a quadratic relation chosen to reproduce the 2π phase shift found at 8.7 mA

heater that may be expected to be proportional to the heater current squared as described by Eq. 10.

$$\Delta\emptyset = \frac{2\pi}{\lambda}\left(\frac{\mathrm{dn}}{\mathrm{dT}}\right)_{\mathrm{si}} \Delta T\, L_H \tag{9}$$

$$P = \mathrm{RI}^2 \tag{10}$$

It shows the phase change induced by the heater may be expected to be linearly proportional relation to the power dissipation and therefore at least quadratic with the injected current. It turns out that a quartic dependence is necessary to fit the MZI data that can be explained by a positive temperature coefficient of resistance of the heater. It was also found that the induced phase change had a slightly greater than linear dependence on the heat dissipated. The optical path length is a

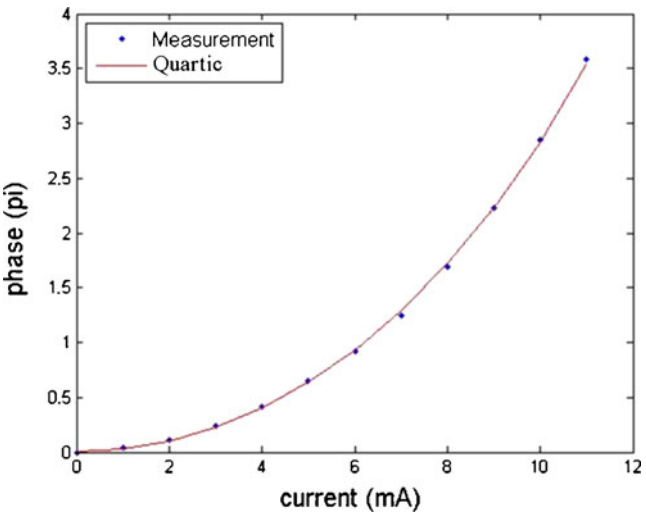

Fig. 7 The curve shows the relation between phase and current (milliampere) for a nonquadratic dependency (quartic)

product of a refractive index and a physical path length. So it may be that the effective length of the thermo-optic modulator also experiences a linear change with temperature due to heat spreading along the waveguide. Thus, their product will generate a quadratic term in the phase change versus power dissipated. The thermo-optic phase change as a function of heater power dissipation is modelled by:

$$\Phi = K_1 P + K_2 P^2 \tag{11}$$

Where K_1 and K_2 relate the induced phase change to the heater power dissipation, P.

But the simplest model neglects the quadratic term in the power dissipation by assuming the heater resistance is constant. In this model, the thermo-optically induced phase change differences Φ is quadratic in the current:

$$\Phi = \beta I^2 \tag{12}$$

Where β is a coefficient, I is the heater current in milliampere and Φ is the relative phase changes. By finding the current required for a 2π phase shift from the transmission characteristics of MZI in Fig.4, the value of β can be calculated and consequently the phase change can be predicted for any current within the assumption of a quadratic dependence. But this approximation is not sufficient to precisely reproduce the MZI data.

In the experiment on the optical array antennas structure, by sweeping the current injected to the heater elements associated to the antenna elements 9 and 10 (Fig. 5) from 0 to 11 mA it is observed that the 2π phase shift occurs at 8.7 mA.

By closer consideration of the behaviour of induced phase versus heater current it is realised that the basic fitting to a quadratic is poor and to a quartic is good and hence the thermo-optically induced phase change is often not well described by a quadratic dependence on heater current or voltage. Figure 6 shows a clear departure from a quadratic relationship at high current when in Eq. 11, K_2 is set to zero.

A nonquadratic (quartic) dependency between the phase induced and the heater current, in contrast, yields an excellent fit to the data (Fig. 7) by considering K_2 as nonzero in Eq. 11. The actual power dissipation of the heater is described properly in terms of a positive linear coefficient of resistance with power dissipation that is consistent with a positive linear temperature coefficient of resistance and a heater temperature linear in power dissipation.

Hence, the transmission studies of Mach–Zenhnder Interferometers with thermo-optic phase tuning sections and far-field beam-steering data from thermo-optically phase tuned OPA devices, both showed that the thermo-optically induced phase is often not well described by a quadratic dependence upon heater current or voltage. It was necessary to add a quartic term to obtain close fits to the obtained data. Physically, in terms of a positive temperature co-efficient of the heater resistance and a linear dependence of induced phase on heater dissipation is enough in most cases to describe this difference from the expected behaviour in the region of operation.

6 Conclusions

In this paper, the characteristics of the far-field radiation pattern and beam steering using a 2D OPA in different kind of structures were verified. The measurements of the beam widths of 2×2, 4×4, and 16×16 structures agreed with theoretical predictions. An error was observed in the measurements methods with an increase in the dimensions of the array which was due to the narrower beam width of the radiation pattern produced by 4×4 and 16×16 structures relative to the size of the pixels of the image sensor. It was realised that the beam steering using a 2D OPA is possible by wavelength tuning with the implemented delay lines. The beam steering observed was −0.16°/nm for 2×2 and 4×4 structures with the same delay lines lengths and spacing elements which agree with the theoretical prediction. Beam steering in a 2D OPA is completed by the thermo-optic beam steering method that exploits the high-temperature coefficient characteristics of silicon in. The thermo-optically induced phase change is often not well described as having a quadratic dependence upon heater current or voltage. It was necessary to add a quartic term to obtain a close fit to the measured data.

Acknowledgments This work was carried out when Ms. Nikkhah was with Photonics Research Group, Ghent University, She is very grateful to Dr. Trevor Hall of the University of Ottawa for his comments and observations.

References

1. McManamon PF, Bos PJ, Escuti MJ, Heikenfeld J, Serati S, Xie HK, Watson EA (2009) A review of phased array steering for narrow-band electrooptical systems. Proc IEEE 97(6):1078–1096
2. Van Acoleyen K, Rogier H, Baets R (2010) Two-dimensional optical phased array antenna on silicon-on-insulator. Opt Express 18(13):13655–13660
3. Van Acoleyen K, Bogaerts W, Jagerska J, Le Thomas N, Houdre R, Baets R (2009) Off-chip beam steering with a one-dimensional optical phased array on silicon-on-insulator. Opt Lett 34(9):1477–1479
4. Roelkens G, Vermeulen D, Van Thourhout D, Baets R, Brision S, Lyan P, Gautier P, Fedeli JM (2008) High efficiency diffractive grating couplers for interfacing a single mode optical fiber with a nanophotonic silicon-on-insulator waveguide circuit. Appl Phys Lett 92(13):131101

5. Van Acoleyen K, Rogier H, Baets R (2009) Feasibility of integrated optical phased arrays for indoor wireless optical links. In: 35th European Conference on Optical Communication 2009 (ECOC '09). Vienna, Austria, p. P4.18
6. Le Thomas N, Houdre R, Kotlyar MV, O'Brien D, Krauss TE (2007) Exploring light propagating in photonic crystals with Fourier optics. J Opt Soc Am B 24(12):2964–2971
7. Green RJ, Joshi H, Higgins MD, Leeson MS (2008) Recent developments in indoor optical wireless systems. IET Commun Mag 2:3–10
8. Chan T, Myslivets E, Ford JE (2008) 2-dimensional beamsteering using dispersive deflectors and wavelength tuning. Opt Express 16 (19):14 617–14 628
9. Nikkhah H, Van Acoleyen K, Baets R (2011) Optical phased arrays in silicon on insulator for optical wireless systems, international symposium on Green Radio over fiber & all Optical technologies for Wireless Access Networks (GROWAN2011). France
10. Van Acoleyen Karel (2011) Hot stuff, technology meeting, January 26th